

Complex Microstructures of Amphiphilic Diblock Copolymer in Dilute Solution

Xuehao He, Haojun Liang,* Lei Huang, and Caiyuan Pan

Department of Polymer Science and Engineering, University of Science and Technology of China, Hefei, Anhui, 230026, P. R. China

Received: July 4, 2003; In Final Form: November 21, 2003

The complex microstructures assembled by amphiphilic diblock copolymer in dilute solution have been investigated by the application of real-space self-consistent field theory in two-dimensional space. Different micelles, such as spherelike micelles, rodlike micelles, and vesicles are produced. The simulations show that vesicles are metastable in dilute solution within a certain range of some parameters. The mechanism for the formation of micromorphologies, especial vesicles, is discussed.

1. Introduction

Previous experiments demonstrated the ability of amphiphilic diblock copolymers to assemble into various complex microstructures in dilute solution. Among these complex microstructures, a specific type, named vesicles, are biologically significant because of their extensive applications in drug delivery systems and artificial cells.¹ It has been experimentally observed that even a simple system like an amphiphilic diblock copolymer can assemble into vesicles and rodlike or spherelike micelles in water depending on manipulation procedures.^{2–5}

Currently, the origin for the formation of these complex microstructures is not clear. Various theoretical approaches, such as coarse-grained surface models,^{6–8} Brownian dynamic simulations,^{9,10} Monte Carlo simulations,^{11,12} and dissipative particle dynamics (DPD) have been used to investigate the formation of vesicles and the dynamic process of self-assembly of amphiphilic molecules.¹³ These methods focused on the self-assembly process of amphiphilic copolymers in a small sample space (only from one to two vesicles formed at final equilibrium). Obviously, it is not known whether the same equilibrium can be obtained for a larger system. The longer computational time cost using a larger sample is beyond tolerance. In addition to the above methods, self-consistent field theory (SCFT), a mesoscopic simulation technique originated by Edwards in the 1960s and adapted by Helfand and others to treat self-assembly of block copolymers,^{14–20} is another approach for exploring spontaneous vesicle formation in dilute solution. This method has been widely applied to study the performance of block copolymer in solution.^{19,20} In addition, another real-space self-consistent field, namely, dynamic density-functional theory (DDFT), was also used to understand the behaviors of block copolymers in solution and to capture the micelle shape and the mechanism of formation.^{21,22} However, all these studies focus on concentrated solutions (in general, polymer concentration >30%). Meanwhile, as a result of lower computation efficiency (for DDFT) and special requirements (in conventional SCFT the symmetry of a mesophase should be specified in advance),²⁵ it is difficult to study dilute solutions and the mechanism for the formation of a bilayer vesicle. In this paper, a real-space SCFT approach developed by Fredrickson's group^{23–25} was applied to the study of the formation of

mesophases of amphiphilic diblock copolymer in dilute solution in two-dimensional (2D) space. The studies are useful for understanding the mechanism for the formation of the complex microstructures of block copolymers, especial vesicles, in dilute solution.

2. Self-Consistent Mean Field Theory and Calculation Algorithm

Amphiphilic diblock copolymers with hydrophobic segments (**A**), hydrophilic segments (**B**), and solvent molecules (**S**) are involved in volume V . The volume fractions of segments **A** and **B** in the system are f_A and f_B , respectively. As a result, the volume fractions of copolymer and solvent in solution are $f_P = f_A + f_B$ and $f_S = 1 - f_P$, respectively. In real-space SCFT one considers the statistics of a single copolymer chain in a set of effective chemical potential fields ω_I , where I represents block species **A** or **B**. These chemical potential fields, which replace the actual interactions between different components, are conjugated to the segment density fields, ϕ_I , of block species I . Similarly, solvent molecules are considered to be in an effective chemical potential field ω_S that conjugates to the solvent density field ϕ_S . Hence, the free energy function (in units of $k_B T$) of the system is given by

$$F = -f_S \ln(Q_S/V) - \frac{f_P}{N} \ln(Q_P/V) + \frac{1}{V} \int dr [\chi_{AB} \phi_A \phi_B + \chi_{AS} \phi_A \phi_S + \chi_{BS} \phi_B \phi_S - \omega_A \phi_A - \omega_B \phi_B - \omega_S \phi_S - P(1 - \phi_A - \phi_B - \phi_S)] \quad (1)$$

where N is the length of the copolymer chain, χ_{ij} is the Flory–Huggins interaction parameter between species i and j , P is the Lagrange multiplier (as a pressure), $Q_S = \int dr \exp(-\omega_S)$ is the partition function of the solvent in the effective chemical potential field ω_S and $Q_P = \int dr q(r,1)$ is the partition function of a single chain in the effective chemical potential fields ω_A and ω_B . The end-segment distribution function $q(r,s)$ gives the probability that a section of a chain, of contour length s and containing a free chain end, has its “connected end” located at r . The parametrization is chosen such that the contour variable s increases continuously from 0 to 1 corresponding from one end of the chain to the other. With the use of a flexible Gaussian chain model to describe the single-chain statistics, the function

* Corresponding author. E-mail: hjiang@ustc.edu.cn.

$q(r,s)$ satisfies a modified diffusion equation.

$$\frac{\partial}{\partial s} q(r,s) = \nabla^2 q(r,s) - N\omega q(r,s) \quad (2)$$

This equation satisfies the initial condition $q(r,0) = 1$. Here, ω is ω_A when $0 < s < 1 - f_A$ and ω_B when $1 - f_A < s < 1$. Similarly, a second distribution function $q'(r,s)$ (containing another chain end) is also satisfied by eq 2 with the initial condition $q'(r,0) = 1$ but in this case ω is ω_B when $0 < s < 1 - f_A$ and ω_A when $1 - f_A < s < 1$. The density of each component is obtained by

$$\begin{aligned} \phi_A(r) &= \frac{1}{Q_P} \int_0^{c_A} ds q(r,s) q'(r,1-s) \\ \phi_B(r) &= \frac{1}{Q_P} \int_{c_A}^1 ds q(r,s) q'(r,1-s) \\ \phi_S(r) &= \frac{\exp(-\omega_S(r))}{Q_S} \end{aligned} \quad (3)$$

Here, c_A is the length fraction of the **A** segments in a copolymer chain. From the equilibrium condition, that is, minimization of the free energy to density and pressure, $\delta F/\delta\phi = \delta F/\delta P = 0$ leads to another four equations.

$$\begin{aligned} \omega_A(r) &= \chi_{AB}(\phi_B(r) - f_B) + \chi_{SA}(\phi_S(r) - f_S) + P(r) \\ \omega_B(r) &= \chi_{AB}(\phi_A(r) - f_A) + \chi_{BS}(\phi_S(r) - f_S) + P(r) \\ \omega_S(r) &= \chi_{SA}(\phi_A(r) - f_A) + \chi_{BS}(\phi_B(r) - f_B) + P(r) \\ \phi_A(r) + \phi_B(r) + \phi_S(r) &= 1 \end{aligned} \quad (4)$$

Here, constant shifts in the potential are introduced in the equations.

The method is to search for low free energy solutions of the equations within a planar square or box with a periodic boundary condition. The initial value of ω is constructed by $\omega_f(r) = \sum_{i \neq j} \chi_{ij}(\phi_i(r) - f_i)$, where f_i represents the average volume fraction of the copolymer segments and solvents and $\phi_i(r) - f_i$ satisfies the Gaussian distributions:

$$\begin{aligned} \langle(\phi_i - f_i)\rangle &= 0 \\ \langle(\phi_i(r) - f_i)(\phi_j(r') - f_j)\rangle &= \beta f_i f_j \delta_{ij} \delta(r - r') \end{aligned} \quad (5)$$

Here, β is defined as the density fluctuation at the initial temperature. The effective pressure field, $P = C_2 C_3(\omega_A + \omega_B) + C_1 C_3(\omega_B + \omega_S) + C_1 C_2(\omega_A + \omega_S)/2(C_1 C_2 + C_2 C_3 + C_1 C_3)$, on each grid is obtained through solving eq 4, where $C_1 = \chi_{SA} + \chi_{BS} - \chi_{AB}$, $C_2 = \chi_{SA} + \chi_{AB} - \chi_{BS}$, and $C_3 = \chi_{AB} + \chi_{BS} - \chi_{SA}$. The density field ϕ_i of species *i*, conjugated to the chemical potential field ω_i , can be evaluated based on eqs 2 and 3. The chemical potential field ω_i can be updated by using the equation $\omega_i^{\text{new}} = \omega_i^{\text{old}} + \Delta t(\delta F/\delta\phi_i)^*$, where $(\delta F/\delta\phi_i)^* = \sum_{M \neq I} \chi_{IM}(\phi_M(r) - f_M) + P(r) - \omega_i^{\text{old}}$ as the chemical potential force. In our simulation, the time step $\Delta t = 0.3$ and the above steps are iterated until the free energy converges to a local minimum, where the phase structure corresponds to a metastable state. This iteration scheme is a pseudodynamics process with a steepest descent on the energy landscape to the nearest metastable solution. It is possible to reach various metastable states depending on the initial conditions.

The numerical simulations were on the two-dimensional space with a 220×220 square lattice with space length $L = 73.333$

and grid size $\Delta x = 0.3333$ in the unit of R_g (unperturbed mean-square radius-of-gyration of a copolymer chain). The sample size selected should be large enough to ensure that the phase morphologies are not a result of the smaller sample space which often produces an artificial phase structure in the melt system. In our experience, using a larger space length and a smaller grid size will cost much time without producing an obvious change in the results. The simulations for each sample are carried out until the phase patterns are stable and invariable with time and $\Delta F < 0.0001$. The simulation of the homogeneous block copolymer solution was reiterated from 10 to ~ 20 times from different initial random states and different random numbers to ensure that the phenomena are not accidental. The critical concentration of polymer chain in solution is expressed as $\rho_V^* = N/\pi R_g^2$, where $R_g = \sqrt{N}$ and N is the chain length; $\rho_V^* = 0.318$ in 2D. In the present simulation, a value of $f_P = 0.1$ ensures that the system is in dilute solution. At the same time, the length of the chain N equals 17 and the length fraction of **B** block c_B equals 0.118 in all simulations.

3. Results and Discussion

In the present simulations, we demonstrate the ability of amphiphilic diblock copolymers to assemble into various complex microstructures (spherulike or rodlike micelles and vesicles) in dilute solution for certain molecular parameters, solvent quality, and manipulation procedures, which have also been observed in experiments.²⁻⁵ We provide, as an example, the microstructural patterns (Figure 1) of diblock copolymers with interaction parameters $\chi_{AB}N = 17.85$, $\chi_{AS}N = 20.4$, and $\chi_{BS}N = -7.65$. In this case, solvent is preferential to block **B**. The microstructural patterns are exhibited in features of solid rodlike and spherulike micelles or vesicles depending on a parameter referred to as the initial density fluctuation amplitude β (detailed analysis of the parameter will be given later). When the solubility of **B** block is disrupted by assigning $\chi_{AB}N = 17.85$, $\chi_{AS}N = 20.4$, $\chi_{BS}N = 0.6373$, a set of microstructural patterns quite different from those in Figure 1, such as solid micelles and experimentally observed compound vesicles,²⁻⁵ are produced (Figure 2). On the other hand, if the solubility of **B** block is improved by assigning $\chi_{AB}N = 17.85$, $\chi_{AS}N = 20.4$, and $\chi_{BS}N = -19.125$, solid micelles and collapsed vesicles are found (Figure 3). For a system with a given block copolymer and solvent quality, the initial density fluctuation amplitude β plays an essential role in determining the final pattern. In fact, the final microstructural patterns in dilute solution are defined by the component density distribution which is mathematically governed by combination of eqs 2, 3, and 4; namely, the component density distribution is a solution of eq 2, 3, and 4. It is reasonable that the different initial conditions defined by eq 5 (β value) should correspond to different solutions (microstructural patterns). In applications of real-space SCFT to concentrated solutions and melts, the dependence of the final microstructures on β is not found because the initial density fluctuation amplitude is so small compared with the original density that its influence on the final patterns can be ignored. However, in the cases of dilute solution, the initial density fluctuation amplitude is comparable to its original density, and the influence of the initial density fluctuation can no longer be ignored. We can conceive that the polymer chains should constantly fluctuate in a homogeneous dilute solution with certain density amplitudes before phase separation. Once phase separation occurs, those preaggregated chains due to density fluctuation should act as a "nucleus", from which phase growth starts. The larger amplitude of concentration fluctuation should

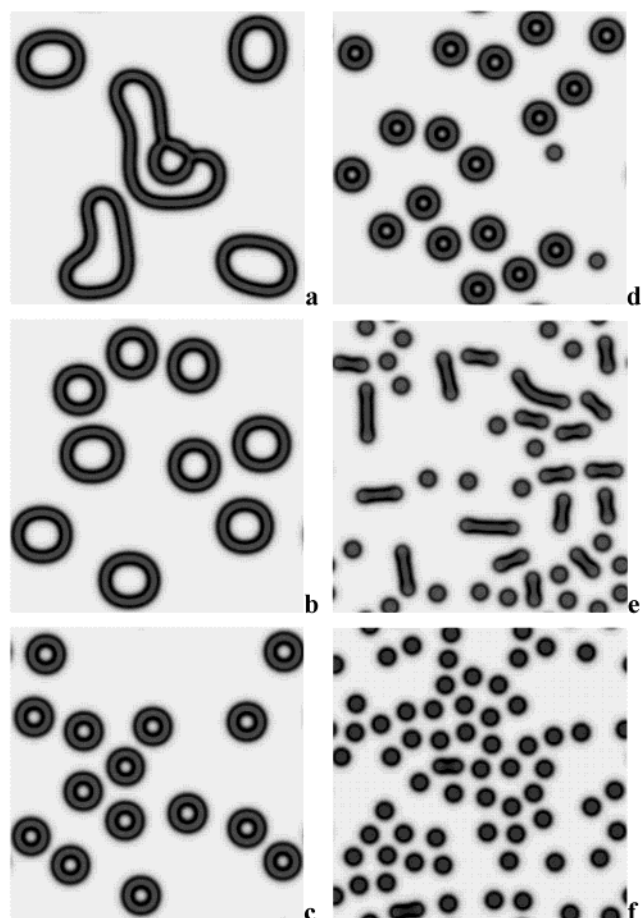


Figure 1. Ordered microphases of amphiphilic diblock copolymer in dilute solution from different values of initial density fluctuation β and relative free energy F , with $\chi_{AB}N = 17.85$, $\chi_{AS}N = 20.4$, $\chi_{BS}N = -7.65$: (a) $\beta = 1.0 \times 10^{-14}$, $F = 0.2926$; (b) $\beta = 1.0 \times 10^{-6}$, $F = 0.2929$; (c) $\beta = 0.0025$, $F = 0.2934$; (d) $\beta = 0.01$, $F = 0.2946$; (e) $\beta = 0.09$, $F = 0.3131$; (f) $\beta = 0.16$, $F = 0.3242$. The gray and black areas are the A and B segments, respectively.

generally correspond to the shorter correlation length, which leads to the spherulike micelle. In contrast, vesicles can be formed by a smaller amplitude of the concentration fluctuation, namely, a longer correlation length. The above process is simulated by randomly assigning initial polymer density fluctuations in solution based on eq 5. The fluctuation amplitude is controlled by parameter β (so referred to as the initial density fluctuation amplitude). For example, in the case of interaction parameters $\chi_{AB}N = 17.85$, $\chi_{AS}N = 20.4$, and $\chi_{BS}N = -7.65$ (Figure 1) and a low initial density fluctuation amplitude such as $\beta = 0.0025$, a number of uniform vesicles are formed (Figure 1c), whereas with an increase of the initial density fluctuation amplitudes to $\beta = 0.09$ and $\beta = 0.16$, solid rodlike and spherulike micelle mixtures (Figure 1e) and pure spherulike micelles (Figure 1f) are produced, respectively.

Analysis of the relative free energies of the systems corresponding to the different micromorphologies in Figures 1 and 2 indicates that those micromorphologies belong to a set of metastable states. For example, in the case of $\chi_{AB}N = 17.85$, $\chi_{AS}N = 20.4$, $\chi_{BS}N = -7.65$, the systems with micromorphologies such as those shown in Figure 1a–f have relative free energies $F = 0.2926$, 0.2929 , 0.2934 , 0.2946 , 0.3131 , 0.3242 . Obviously, in each case the system does not correspond to the lowest free energy. The system is believed to have been trapped in different high free energy states, that is, in a set of metastable states. This explains why different micromorphologies for a

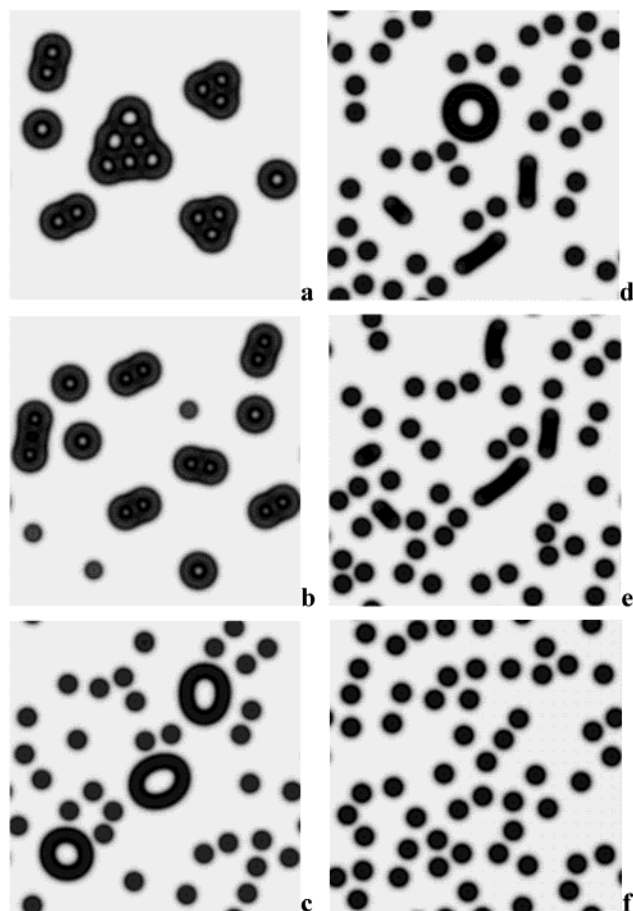


Figure 2. Ordered microphases of amphiphilic diblock copolymer in dilute solution from different values of initial density fluctuation β and relative free energy F , with $\chi_{AB}N = 17.85$, $\chi_{AS}N = 20.4$, $\chi_{BS}N = 0.6375$: (a) $\beta = 1.0 \times 10^{-16}$, $F = 0.2622$; (b) $\beta = 1.0 \times 10^{-6}$, $F = 0.2679$; (c) $\beta = 0.04$, $F = 0.2935$; (d) $\beta = 0.0625$, $F = 0.2990$; (e) $\beta = 0.09$, $F = 0.3052$; (f) $\beta = 0.16$, $F = 0.3099$. The gray and black areas are the A and B segments, respectively.

given block copolymer in dilute solution can be produced by different manipulation procedures in experiments. These metastable states strongly depend on the pathways on the free energy landscapes, which are controlled by experimental conditions, and correspond to the initial density fluctuations in our simulations.

The evolution processes of segregation of the system with $\chi_{AB}N = 17.85$, $\chi_{AS}N = 20.4$, and $\chi_{BS}N = -7.65$ and the different initial density fluctuations $\beta = 0.0025$ and $\beta = 0.16$ are shown in Figures 4 and 5. We notice from the simulated trajectory that at low initial density fluctuation amplitude most “nuclei” are unstable; they redissolve into solvent instead of grow. After longer time organizations ($t = 33$, 110 iteration steps in the case of $\beta = 0.0025$), a few stable “nuclei” are established. In contrast, at high initial density fluctuation amplitude many stable “nuclei” are quickly formed ($t = 0.6$, 2 iteration steps in the case of $\beta = 0.16$), that is, they cannot redissolve easily. In the case of low $\beta = 0.0025$ (Figure 4), the component density profile in the first “nucleus” that appeared at $t = 33$ (Figure 4a) is in the feature of a single peak, that is, both the hydrophobic and the hydrophilic segment density reduces from the nucleus’ center to the periphery, whereas the solvent in the central region of nucleus remains high density. By further evolution, more hydrophobic segments aggregate in the “nucleus”, which leads to the decrease of solvent density in that area due to the repulsive force of the hydrophobic segment

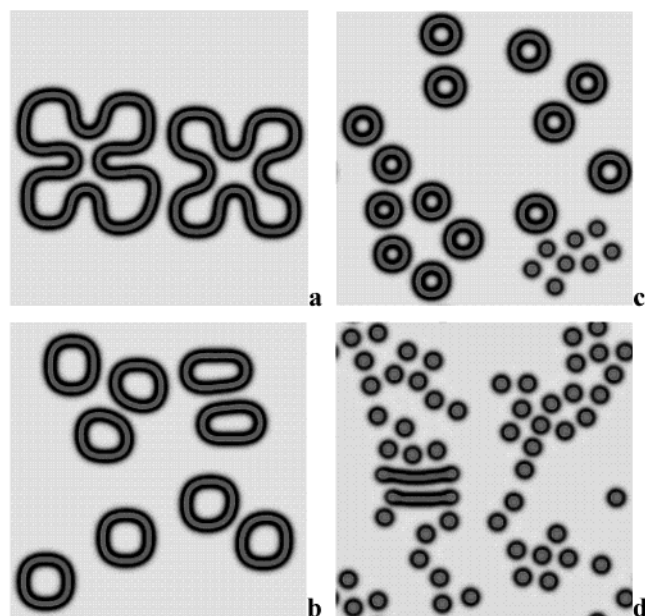


Figure 3. Ordered microphases of amphiphilic diblock copolymer in dilute solution from different values of initial density fluctuation β and relative free energy F , with $\chi_{AB}N = 17.85$, $\chi_{AS}N = 20.4$, $\chi_{BS}N = -19.125$: (a) $\beta = 0.0225$, $F = 0.3115$; (b) $\beta = 0.04$, $F = 0.3105$; (c) $\beta = 0.0625$, $F = 0.3121$; (d) $\beta = 0.09$, $F = 0.3345$. The gray and black areas are the A and B segments, respectively.

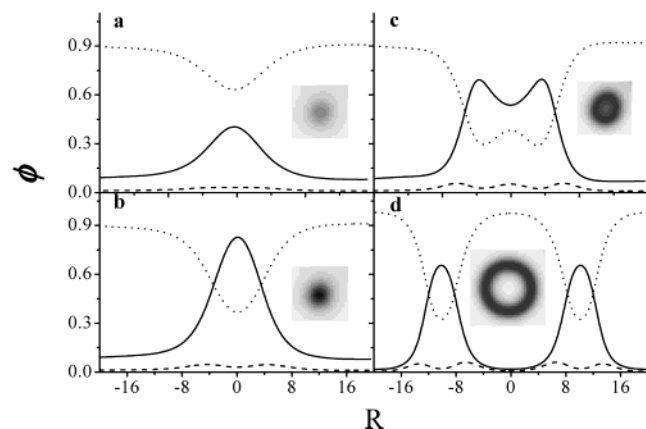


Figure 4. Density distributions ϕ of A (hydrophobic segment, solid line), B (hydrophilic segment, dash line), and S (solvent, dash dot line) along the radius direction of a vesicle in Figure 1c at different times during the evolution: (a) $t = 33$, (b) $t = 36$, (c) $t = 45$, (d) equilibrium state. The density distribution of the copolymer is shown in the small picture.

to the solvent (Figure 4b). It is worth noticing that the hydrophilic segments at the central areas of the nucleus remain in high density, which has the ability to attract solvent into the nucleus. Then, the hydrophobic segment density profile splits into double peaks (Figure 4c), indicating that the hydrophobic segment density at the center of the “nucleus” decreases while both the solvent and the hydrophilic density increase. Finally, a bilayer vesicle is formed in which the solvents fully occupy the center (Figures 1c and 4d). In comparison, the hydrophobic segments in the high- β case can easily aggregate in the central area of the “nucleus” (Figure 5a). Consequently, the density profile of the hydrophilic segment has double peaks without hydrophilic segments in the central region. In fact, a solid micelle is generated. With phase evolution, these solid micelles grow without changing their structures and lead to the final micelles as show in Figures 1f and 5d.

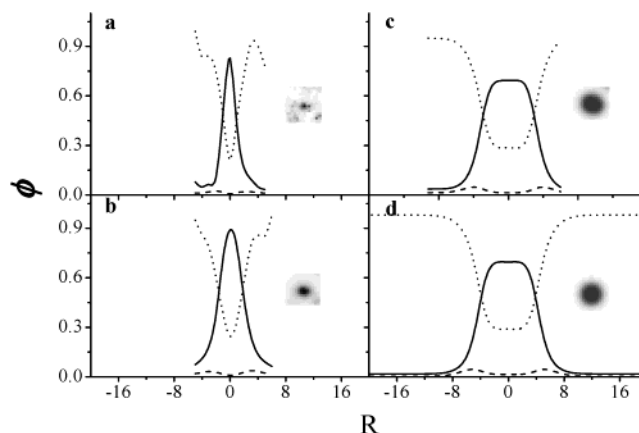


Figure 5. Density distributions ϕ of A (hydrophobic segment, solid line), B (hydrophilic segment, dash line), and S (solvent, dash dot line) along the radius direction of a spherulike micelle in Figure 1f at different times during the evolution: (a) $t = 0.6$, (b) $t = 3.6$, (c) $t = 21$, (d) equilibrium state. The density distribution of the copolymer is shown in the small picture.

The above results suggest that the vesicle is a metastable structure. The key to formation of the vesicle is that a part of the hydrophilic segments exists in the central region of the initial “nucleus”. These hydrophilic segments have the ability to attract solvents into the center of the micelles. The region then further develops into the vesicle or other complex vesicles. The different initial density fluctuations result in the different nucleus structures. In experiments, control of the polymer density fluctuation in solution can be realized by changing the rate of addition of nonsolvent to the dilute solution.

4. Conclusion

Real-space self-consistent field theory was applied to study phase morphologies of amphiphilic diblock copolymer in dilute solution. The preliminary results in two-dimensional space show that the vesicle is metastable. Meanwhile, a number of microstructures, such as compound vesicles, bilayer vesicles, rodlike micelles, and so forth, can form. Their formation strongly depends on the nucleation structure that resulted from the initial density fluctuation.

Acknowledgment. The financial support of the National Science Foundation of China (Grants 20374050 and 50173025) and the Foundation of USTC is gratefully acknowledged.

References and Notes

- (1) Discher, D. E.; Eisenberg, A. *Science* **2002**, 297, 967–973.
- (2) Zhang, L.; Eisenberg, A. *Science* **1995**, 268, 1728–1731.
- (3) Zhang, L.; Yu, K.; Eisenberg, A. *Science* **1996**, 272, 1777–1779.
- (4) Zhang, L.; Eisenberg, A. *Macromolecules* **1996**, 29, 8805–8815.
- (5) Luo, L.; Eisenberg, A. *Langmuir* **2001**, 17, 6804–6811.
- (6) Lipowsky, R. *Nature* **1991**, 349, 475–481.
- (7) Jülicher, F.; Lipowsky, R. *Phys. Rev. Lett.* **1993**, 70, 2964–2967.
- (8) Umeda, T.; Nakajima, H.; Hotani, H. *J. Phys. Soc. Jpn.* **1998**, 67, 682–688.
- (9) Noguchi, H.; Takasu, M. *Phys. Rev. E* **2001**, 64, 041913.
- (10) Noguchi, H.; Takasu, M. *J. Chem. Phys.* **2001**, 115, 9547–9551.
- (11) Bernardes, A. T. *J. Phys. II* **1996**, 6, 169–174.
- (12) Bernardes, A. T. *Langmuir* **1996**, 12, 5763–5767.
- (13) Yamamoto, S.; Maruyama, Y.; Hyodo, S.-A. *J. Chem. Phys.* **2002**, 116, 5842–5849.
- (14) Edwards, S. F. *Proc. Phys. Soc.* **1965**, 85, 613–624.
- (15) Helfand, E. *J. Chem. Phys.* **1975**, 62, 999–1005.
- (16) Matsen, M. W.; Schick, M. *Phys. Rev. Lett.* **1994**, 72, 2660–2663.
- (17) Noolandi, J.; Shi, A.-C.; Linse, P. *Macromolecules* **1996**, 29, 5907–5919.
- (18) Bohbot-Raviv, Y.; Wang, Z. G. *Phys. Rev. Lett.* **2000**, 85, 3428–3431.

- (19) Riess, G. *Prog. Polym. Sci.* **2003**, 28, 1107–1170.
- (20) Linse, P. Modelling of the Self-Assembly of Block Copolymers in Solution. In *Amphiphilic Block Copolymers*; Alexandridis, P., Lindman, B., Eds.; Elsevier: Amsterdam, 2000; pp 13–40.
- (21) van Vlimmeren, B. A. C.; Maurits, N. M.; Zvelindovsky, A. V.; Sevink, G. J. A.; Fraaije, J. G. E. M. *Macromolecules* **1999**, 32, 646–656.
- (22) Guo, S. L.; Hou, T. J.; Xu, X. J. *J. Phys. Chem. B* **2002**, 106, 11397–11403.
- (23) Drolet, F.; Fredrickson, G. H. *Phys. Rev. Lett.* **1999**, 83, 4317–4320.
- (24) Drolet, F.; Fredrickson, G. H. *Macromolecules* **2001**, 34, 5317–5324.
- (25) Fredrickson, G. H.; Ganesan, V.; Drolet, F. *Macromolecules* **2002**, 35, 16–39.
- (26) deGennes, P. G. *Scaling Concepts in Polymer Physics*; Cornell University Press: Ithaca, NY, 1979.